

Kondo effect and spin-polarized transport through a quantum dot with Rashba spin-orbit interaction

Hai-Feng Lü* and Yong Guo†

Department of Physics and Key Laboratory of Atomic and Molecular NanoSciences, Ministry of Education, Tsinghua University, Beijing 100084, People's Republic of China

(Received 7 December 2006; revised manuscript received 29 May 2007; published 30 July 2007)

By using the finite- U slave-boson approach, we study theoretically the spin accumulation, spin-dependent transport, and the shot noise in a magnetic semiconductor quantum dot induced by the Rashba spin-orbit interactions (SOI) in the Kondo regime. It is shown that the Rashba SOI causes the splitting of the Kondo peak and more conductance dips appear in the Fano-type conductance. The spin-polarized conductance indicates two peaks locating both sides of $\epsilon_d = -U/2$ (ϵ_d and U represent the dot level and the Coulomb repulsion, respectively). In the large bias limit and ignoring the effect of Rashba SOI, the Fano factor can be tuned by the direct coupling between two leads while not related to the Coulomb repulsion. It is found that the Rashba SOI can increase or decrease the Fano factor, which depends on the dot level and the chemical potentials in both leads. When the dot level is below the chemical potentials, the Fano factor increases in the presence of Rashba SOI; otherwise, the Rashba SOI suppresses the Fano factor.

DOI: 10.1103/PhysRevB.76.045120

PACS number(s): 72.25.Dc, 73.63.Nm, 72.70.+m

I. INTRODUCTION

The electron spin is considered as an ideal candidate for the qubit to realize the quantum computing in the future.¹ It is an important issue how to control and utilize the spin to realize the spin-polarized accumulation and transportation in semiconductor spintronics. For a mesoscopic quantum dot (QD) system, it is a natural idea to couple with ferromagnetic (FM) leads or use magnetic field to produce and manipulate the spin current.^{2,3} However, these two methods have been considered difficult to realize in a real system. The polarized spins in the FM lead are difficult to inject into a semiconductor, and for the second proposal, one has to confine a strong magnetic field to such a small region of a quantum dot.⁴ So, it will be useful to realize spin-polarized transport just using the intrinsic property of the quantum dot but not with the help of complex experimental conditions. Recently, some theoretical and experimental studies are proposed to improve the efficiency of spin polarization in transport systems based on the spin-orbit interactions (SOI).⁵⁻⁸

Recently, an Aharonov-Bohm (AB) ring device, in which a QD having Rashba SOI is located in one arm, is proposed to realize the spin-polarized transport and spin accumulation.⁶ The device can be considered as the minimum model to realize the spin-polarized transport based on Rashba SOI in a QD system. It is very similar to another widely studied device where a common QD is embedded in an AB ring, while the AB phase is related to spin in the present case. In this modified AB device, interference between the localized states in the QD and the continuous states in the direct coupling between two leads can cause asymmetric Fano resonance peaks in the conductance.⁹ At the same time, the diluted magnetic impurities in the QD can also induce the Kondo effect at low temperature, which has become a long-standing issue in the condensed matter physics.¹⁰ With the rapid development in nanoelectronics, many kinds of QD devices have been subtly designed to show and measure the Kondo effect,¹¹⁻¹⁴ which plays an important role on the

transport properties at low temperature.¹⁵⁻¹⁷ The coexistence of the Fano resonance, the Kondo effect, and the spin polarization in the present device is expected to yield interesting transport phenomena.¹⁸

Except for the spin current, the current noise characteristics in a mesoscopic transport system have been paid much attention in recent years.¹⁹⁻²⁶ The shot noise is caused by the discreteness of charge particles and is unavoidable even at zero temperature. The spectrum of the shot noise can yield some information related to charge fluctuations and is an important tool for studying correlations induced by different types of interactions, which cannot be obtained only through measuring the current. If there is no correlation between carriers, the current fluctuation is described by a Poissonian distribution $S=2eI$. For electron transport in the macroscopic device, the current fluctuation is sensitively affected by the Coulomb repulsion and the Pauli exclusion principle, thus, the shot noise can be enhanced or suppressed with respect to the Poissonian value. One usually introduces the Fano factor $F=S/2eI$ to represent the deviation from Poissonian shot noise for which $F=1$. For a spin-polarized transport system, it has been revealed that the magnetic field can enhance the Fano factor.^{20,21} However, researches on the impact of Rashba SOI on the noise properties are still scarce.

The finite- U slave-boson approach was firstly improved by Kotliar and Ruckenstein to deal with the Anderson single impurity model about 20 years ago.²⁷ Recently, this method is introduced to study the transport through the quantum dot systems in the finite- U case and Kondo regime.²⁸ Together with nonequilibrium Green's function techniques, such an approach allows us to obtain a set of closed formulas self-consistently. Different from well-known Coleman's slave-boson approach,²⁹ this method gives a well description of the transport through QDs with arbitrary strength of Coulomb interaction. Moreover, the Kondo effect can be taken into account and more information can be obtained. To date, it has been successfully applied to some spin-polarized transport cases, such as under the magnetic field, coupled with a

ferromagnetic lead and so on.^{30–32} The results obtained from this method show well agreement with the results from numerical renormalized group technique and the experiments.¹⁶ The finite- U slave-boson approach can be considered as a powerful tool to investigate the spin-polarized transport in a QD system.

In the present paper, we use the finite- U slave-boson approach to study the spin current and its shot noise in a quantum dot induced by Rashba SOI in the Kondo regime. In Sec. II, we give the theoretical framework and the self-consistent equations for the present model. In Sec. III, we study the spin-dependent transport properties numerically. Finally, Sec. IV gives the summary.

II. THEORETICAL FRAMEWORK

We consider a modified AB ring system⁶ where a QD is embedded in one arm. The QD contains the Rashba SOI and there is no Rashba interaction on the other arm of the ring. The ring is connected to the outside world by two normal metal leads. When a voltage V is applied across two leads, a spin-polarized current flows through the QD. The Hamiltonian of the system can be written as

$$H = H_L + H_R + H_D + H_T. \quad (1)$$

Here,

$$H_\alpha = \sum_{k,s} \epsilon_{\alpha k} c_{\alpha k s}^\dagger c_{\alpha k s} \quad (2)$$

stands for the left ($\alpha=L$) or the right ($\alpha=R$) lead with electron energy $\epsilon_{\alpha k}$ and $s(=\uparrow\downarrow)$ is the spin index;

$$H_D = \sum_s \epsilon_d c_{ds}^\dagger c_{ds} + U c_{d\uparrow}^\dagger c_{d\uparrow} c_{d\downarrow}^\dagger c_{d\downarrow} \quad (3)$$

describes the QD with a single orbital level ϵ_d and a finite on-site Coulomb repulsion U between electrons; and

$$H_T = \sum_{k,s} t_{LR} (c_{Lks}^\dagger c_{Rks} + c_{Rks}^\dagger c_{Lks}) + \sum_{k,s} (t_{Ld} c_{Lks}^\dagger c_{ds} + t_{Rd} e^{-isk_R L} c_{Rks}^\dagger c_{ds} + \text{H.c.}) \quad (4)$$

describes the tunneling among the QD, the left lead, and the right lead. The extra spin-dependent phase $sk_R L = s\alpha_R m^* L/\hbar^2$ is generated in the path by Rashba SOI,⁶ with α_R the Rashba SOI strength and L the size of the QD. It should be pointed out that a unitary transformation is introduced to second quantize the Rashba SOI. The above Hamiltonian is derived in a rotating frame which follows the spin precession and then the spin is invariant. If a finite bias voltage is applied, the multilevel QD system with Rashba SOI can exhibit non-Abelian gauge structures, which often give finite non-Abelian Berry phases (also called matrix Berry phase).⁷ Recently, the matrix Berry phases in real space are calculated and the possible testing scheme is also proposed in n -type semiconductor quantum dots with the Rashba and Dresselhaus SOI.^{7,8} A matrix Berry phase represents the mixing between degenerate levels. When the applied bias voltage or the dot-lead coupling is much smaller than the energy

spacing between the QD levels, the effect of the matrix Berry phase is ignorable and the second-quantized Hamiltonian [Eq. (1)] can be considered as a reliable approximation (see the Appendix). In this paper, it is considered that there is only single energy level in the QD, so the change caused by Rashba SOI in the second-quantized Hamiltonian is the extra spin-resolved phase $isk_R L$.

According to the finite- U slave-boson approach, one can use additional four auxiliary boson operators e , $p_s (s=\pm 1)$, and d , which are associated with the empty, singly occupied, and doubly occupied electron states of the QD, respectively. These operators can be used to describe the above physical problem without interparticle coupling in an enlarged space with constraints: the completeness relation $\sum_s p_s^\dagger p_s + e^\dagger e + d^\dagger d = 1$ and the particle number conservation condition $c_{ds}^\dagger c_{ds} = p_s^\dagger p_s + d^\dagger d$ ($s=\pm 1$). Within the mean-field scheme, we start with the following effective Hamiltonian:

$$H_{\text{eff}} = \sum_{k,s,\alpha} \epsilon_{\alpha k} c_{\alpha k s}^\dagger c_{\alpha k s} + \sum_s \epsilon_d c_{ds}^\dagger c_{ds} + U d^\dagger d + \sum_{k,s} t_{LR} (c_{Lks}^\dagger c_{Rks} + c_{Rks}^\dagger c_{Lks}) + \sum_{k,s} (t_{Ld} c_{Lks}^\dagger c_{ds} z_s + t_{Rd} e^{-isk_R L} c_{Rks}^\dagger c_{ds} z_s + \text{H.c.}) + \lambda^{(1)} \left(\sum_s p_s^\dagger p_s + e^\dagger e + d^\dagger d - 1 \right) + \sum_s \lambda_s^{(2)} (c_{ds}^\dagger c_{ds} - p_s^\dagger p_s - d^\dagger d), \quad (5)$$

where three Lagrange multipliers $\lambda^{(1)}$ and $\lambda_s^{(2)}$ ($s=\uparrow\downarrow$) are introduced to take account of the constraints, and in the hopping term, the QD fermion operators c_{ds}^\dagger and c_{ds} are expressed as $z_s^\dagger c_{ds}^\dagger$ and $c_{ds} z_s$ to recover the many-body effect on tunneling. z_s consists of all boson operator sets that are associated with the physical process with which a spin s electron is annihilated:

$$z_s = (1 - d^\dagger d - p_s^\dagger p_s)^{-1/2} (e^\dagger p_s + p_s^\dagger d) (1 - e^\dagger e - p_s^\dagger p_s)^{-1/2}. \quad (6)$$

From the effective Hamiltonian (5), one can derive four equations of motion of slave-boson operators, which, together with the three constraints, serve as the basic equations. Then, we can use the mean-field approximation in the statistical expectations of these equations, in which all the boson operators are replaced by their expectation values. In the wide-band limit for the leads, the resulting equations are as follows:

$$\sum_s |p_s|^2 + |e|^2 + |d|^2 = 1, \quad (7)$$

$$\langle c_{ds}^\dagger c_{ds} \rangle = |p_s|^2 + |d|^2, \quad s = \pm 1, \quad (8)$$

$$\sum_s \frac{\partial z_s}{\partial e} (K_{Ls} + K_{Rs}) + 2\lambda^{(1)} e = 0, \quad (9)$$

$$\sum_{s'} \left(\frac{\partial z_{s'}}{\partial p_s} + \frac{\partial z_{s'}}{\partial p_s^\dagger} \right) (K_{Ls'} + K_{Rs'}) + 2[\lambda^{(1)} - \lambda_s^{(2)}] p_s = 0, \quad (10)$$

$$s = \uparrow \downarrow,$$

and

$$\sum_s \frac{\partial z_s}{\partial d} (K_{Ls} + K_{Rs}) + 2[U + \lambda^{(1)} - \sum_s \lambda_s^{(2)}] d = 0. \quad (11)$$

Here,

$$K_{Ls} = t_{Ld} \langle \sum_k c_{Lks}^\dagger c_{ds} \rangle + t_{Ld} \langle \sum_k c_{ds}^\dagger c_{Lks} \rangle, \quad (12)$$

while

$$K_{Rs} = t_{Rd} e^{-isk_R L} \langle \sum_k c_{Lks}^\dagger c_{ds} \rangle + t_{Rd} e^{isk_R L} \langle \sum_k c_{ds}^\dagger c_{Lks} \rangle. \quad (13)$$

The expressions of K_{Ls} and K_{Rs} can be obtained by calculating the Keldysh Green's function $G^<(\omega)$.

The quantum transport problem described by the effective Hamiltonian can be solved by standard many-body techniques. The expected values appear in the self-consistent equations and all physical quantities discussed below can be calculated by using the standard Keldysh nonequilibrium Green's function method.^{6,28} In the following discussion, we set $\varphi = k_R L$ to describe the spin precession angle caused by Rashba SOI. Before the numerical results are presented, a qualitative analysis may be helpful to understand the spin broken symmetry in the present system. The effective couplings between the QD and the leads can be expressed as¹⁵

$$T_{Ls} = |t_{Ld} - i\pi\rho t_{LR} t_{Rd} e^{is\varphi}|^2 = |t_{Ld}|^2 + |\pi\rho t_{LR} t_{Rd}|^2 + 2\pi\rho t_{Ld} t_{LR} t_{Rd} \sin s\varphi, \quad (14a)$$

$$T_{Rs} = |t_{Rd} e^{is\varphi} - i\pi\rho t_{Ld} t_{LR}|^2 = |t_{Rd}|^2 + |\pi\rho t_{Ld} t_{LR}|^2 - 2\pi\rho t_{Ld} t_{LR} t_{Rd} \sin s\varphi, \quad (14b)$$

where ρ is the density of state in the leads. For $0 < \varphi < \pi$, the spin-up electron is easier to tunnel from the left lead to the QD than the spin-down electron, but it is more difficult for it to tunnel out from the QD to the right lead. Therefore, there is spin accumulation in the QD and the total current is spin polarized.

The retarded Green's functions \mathbf{G}_s^r can be obtained by using the Dyson equation $\mathbf{G}_s^r = \mathbf{g}_s^r + \mathbf{g}_s^r \Sigma_s^r \mathbf{G}_s^r$. Here, \mathbf{g}_s^r is the Green's function of the system without coupling between the leads and the QD (i.e., when $t_{LR} = t_{Ld} = t_{Rd} = 0$) and can be obtained as

$$\mathbf{g}_s^r(\omega) \equiv \begin{pmatrix} -i\pi\rho & 0 & 0 \\ 0 & -i\pi\rho & 0 \\ 0 & 0 & g_{dds}^r(\omega) \end{pmatrix}, \quad (15)$$

where $g_{dds}^r(\omega) = 1/(\omega - \epsilon_{ds}^-)$, with $\tilde{\epsilon}_{ds} = \epsilon_d + \lambda_s^{(2)}$. The self-energy $\Sigma_s^r(\omega)$ can be written as

$$\Sigma_s^r(\omega) \equiv \begin{pmatrix} 0 & t_{LR} & t_{Lds} \\ t_{LR} & 0 & t_{Rds} e^{-is\varphi} \\ t_{Lds} & t_{Rds} e^{is\varphi} & 0 \end{pmatrix}, \quad (16)$$

where $t_{Lds} = t_{Ld} z_s$ and $t_{Rds} = t_{Rd} z_s$. From Eqs. (15) and (16), \mathbf{G}_s^r can be obtained by solving Dyson's equation $\mathbf{G}_s^r = (\mathbf{g}_s^{r-1} - \Sigma_s^r)^{-1}$. Then, after solving $\mathbf{G}_s^r(\omega)$, we can calculate the less Green's function $\mathbf{G}^<(\omega)$ straightforwardly.

III. NUMERICAL RESULTS AND DISCUSSIONS

In this section, we discuss the spin accumulation, spin-dependent transport, and the shot noise properties for the QD system. We suppose that the left and right leads are made from the identical material and assume constant effective coupling strength in the wide-band limit, $\Gamma_{Ls}(\omega) = \Gamma_{Rs}(\omega) = \Gamma_s$ for both spin-up and spin-down orientations. Following the former studies,⁶ we take the density of states ρ in the leads as the energy units and take symmetric coupling strengths as $t_{Ld} = t_{Rd} = 0.4$ (the corresponding linewidth $\Gamma = 2\pi\rho |t_{L(R)d}|^2 \approx 1$) in the whole paper. When an external voltage V is applied between the two leads, the corresponding chemical potential is taken as $\mu_L = -\mu_R = V/2$.

A. Spin accumulation in the QD

Under the framework of slave-boson approach, the four slave Bose fields can be assumed as c numbers and replaced by their corresponding expectation values. One can obtain the possibilities of four states in the QD and from which the spin accumulation in the QD can be defined as $\Delta_n \equiv p_\uparrow^2 - p_\downarrow^2$, where p_\uparrow^2 and p_\downarrow^2 represent the possibilities of single spin-up occupied and single spin-down occupied, respectively.

First, we consider the case where the e-e Coulomb repulsion is ignored (i.e., $U=0$). Figure 1(a) gives an illustration how the possibilities of the four states change with the energy level in the QD. As expected, possibility of the spin-irrelevant state and empty (double occupied) state e^2 (d^2) increases (decreases) with the increase of ϵ_d and approaches to 1 in the limit of high (low) level ϵ_d . In the presence of Rashba SOI, the possibilities of two spin-dependent states p_\uparrow^2 and p_\downarrow^2 are not equivalent anymore. Figure 1(b) illustrates the dependence of the spin accumulation Δ_n on the dot energy level ϵ_d for different Coulomb interactions $U=0.0, 5.0$, and 10.0 . For $U=0.0$, two peaks lie on two sides of the Fermi energy, which are also not symmetric about $\epsilon_d=0$. However, only one symmetric peak appears at $\epsilon_d=0$ where the Kondo effect is ignored in the former studies.⁶ The possible reason is that different pictures are taken in two treatments: the direct electronic creation and annihilate operators are taken for the QD in the former work, while here the states in the QD are taken as the basis vectors. For the finite U , the spin accumulation has slightly improved and $\Delta_n \sim \epsilon_d$ curve has the same shape as the case of $U=0$. The valley between the two polarized peaks locates near $\epsilon_d = -U/2$, which is consistent with the former study.⁶ In Fig. 2, we present the dependence of the spin accumulation Δ_n versus the dot level ϵ_d for different Rashba strengths $\varphi=0.0, 0.2$, and 0.4 . With the increase of φ , Δ_n increases but the positions of the peaks do

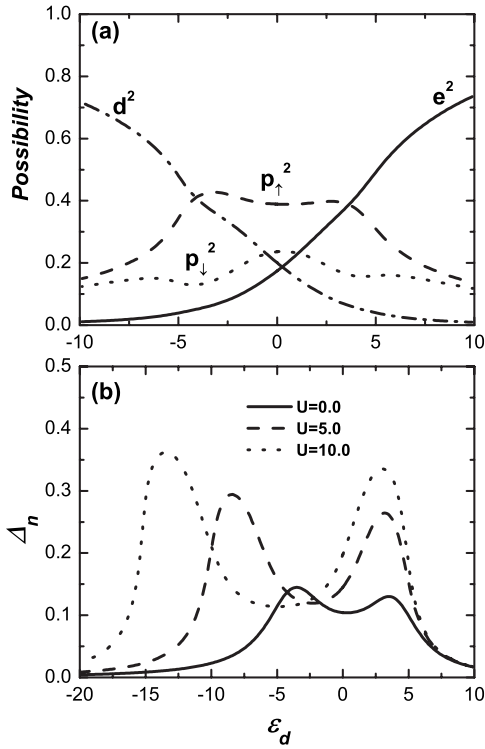


FIG. 1. (a) The possibilities of the four states p_\uparrow^2 , p_\downarrow^2 , e^2 , and d^2 as a function of the dot level ϵ_d for $U=0.0$, $t_{LR}=0.1$, $\varphi=0.2$, and $V=2.0$. (b) The spin polarization Δ_p as a function of ϵ_d for $U=0.0$, 5.0, and 10.0. The other parameters are $V=3.0$, $t_{LR}=0.1$, and $\varphi=0.2$.

not change. Moreover, the spin accumulation approaches to zero in the large or small limit of the dot level ϵ_d . The reason is that the dot is dominated by empty state or doubly occupied state in both limits. Therefore, only in the middle region between the two limits the Rashba SOI has remarkable effects on the spin-polarized transport.

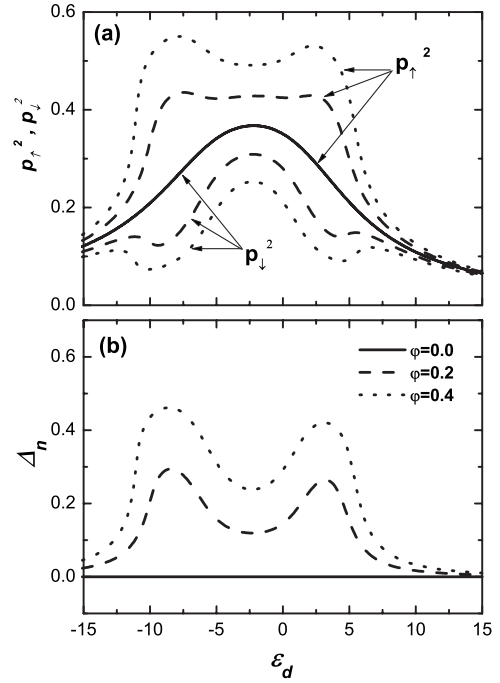


FIG. 2. (a) The possibilities p_\uparrow^2 and p_\downarrow^2 . (b) The spin polarization in the QD Δ_p as a function of the dot level ϵ_d for $\varphi=0.2, 0.4$, and 0.6 . The other parameters are $U=5.0$, $t_{LR}=0.1$, and $V=3.0$.

B. Spin-dependent differential conductance

By applying the Landauer formula in the steady state, the current flowing through the system, contributed by spin-up or spin-down electrons, can be derived as^{22,23}

$$I_s = \frac{e}{h} \int d\omega [f_L(\omega) - f_R(\omega)] T_s(\omega), \quad (17)$$

where $f_\alpha(\omega)$ denotes the Fermi distribution function for electrons in the α electrode and the transmission probability is given by

$$T_s(\omega) = \frac{2}{\pi^2 \rho^2} \frac{t_{LR}^2 g_{dds}^r{}^{-1}(\omega) + 2t_{LR}t_{Lds}t_{Rds} \cos s\varphi g_{dds}^r{}^{-1}(\omega) + t_{Lds}^2 t_{Rds}^2}{\Lambda(\omega)}, \quad (18)$$

with

$$\Lambda(\omega) = \left[\frac{g_{dds}^r{}^{-1}(\omega)}{\pi^2 \rho^2} + t_{LR}^2 g_{dds}^r{}^{-1}(\omega) + 2t_{LR}t_{Lds}t_{Rds} \cos s\varphi \right]^2 + \frac{(t_{Lds}^2 + t_{Rds}^2)^2}{\pi^2 \rho^2}. \quad (19)$$

From Eq. (17), one can obtain the components of conductance $G_s = dI_s/dV$, the total conductance $G = \sum_s dI_s/dV$, and the spin-polarized conductance $G_p = G_\uparrow - G_\downarrow$.

In this section, we focus on the case with a finite bias voltage. Actually, it has been proved that there is no spontaneous spin symmetry broken at equilibrium case.⁶ For $V=0$, the spin-resolved phase caused by Rashba SOI

has the same effects as the magnetic flux in an AB ring with a common dot. The recent experiments show the suppression of the Kondo plateau by the Fano resonance for large on-site Coulomb repulsion U .^{13,14} For the case with finite bias voltage, spin up and spin down are not equilibrium anymore and spin current can be induced by the Rashba SOI.

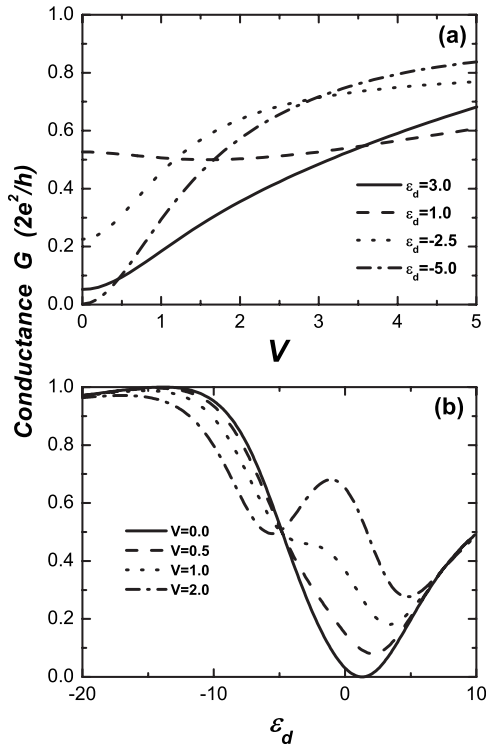


FIG. 3. (a) The conductance G vs the bias V for different dot levels ϵ_d in the absence of Rashba SOI ($\varphi=0$): $\epsilon_d=3.0, 1.0, -2.5$, and -5.0 . $U=5.0$ and $t_{LR}=0.2$. (b) The conductance G versus dot level ϵ_d for different biases V : $V=0.0, 0.5, 1.0$, and 2.0 . $U=5.0$ and $t_{LR}=0.2$.

The conductance of a normal QD embedded in an AB ring has been widely studied numerically and analytically.^{16,17,22,26} Compared with the former studies, we first present the results without taking φ into account, as shown in Fig. 3. Figure 3(a) shows the conductance as a function of the bias voltage V for different energy levels ϵ_d . Figure 3(b) shows the dependence of the conductance on the dot level ϵ_d for various biases $V=0.0, 0.5, 1.0$, and 2.0 . A Fano-Kondo plateau in the conductance is formed due to the bias voltage, while this plateau only appears for large on-site Coulomb repulsion U in the equilibrium case $V=0$.¹⁷ As V increases further, a Kondo-type conductance peak appears near the Fermi energy and so there are two resonance dips in the Fano-type conductance, which accords the experiment results.^{11,14}

Figure 4 illustrates the spin-dependent conductance G_s , total conductance $G=G_\uparrow+G_\downarrow$, and the spin-polarized conductance $G_p=G_\uparrow-G_\downarrow$ versus the bias voltage V . For different Rashba interaction strengths $\varphi=0, 0.2, 0.5$, and 1.0 , the total conductance G approaches the same value in the large V limit. In the linear response case, the total conductance increases gradually with the increase of φ , where φ tunes the coherent phase like a magnetic flux in the common AB ring. Furthermore, as the Rashba SOI strength increases, the polarized conductance appears and shows peaks with the increase of bias voltage V [see Fig. 4(c)]. For relatively small $\varphi=0.2$, there are two peaks in $G_p \sim V$ curve. These two peaks start from the small and large limits of V and become close with each other as the φ increases. Eventually, there is only

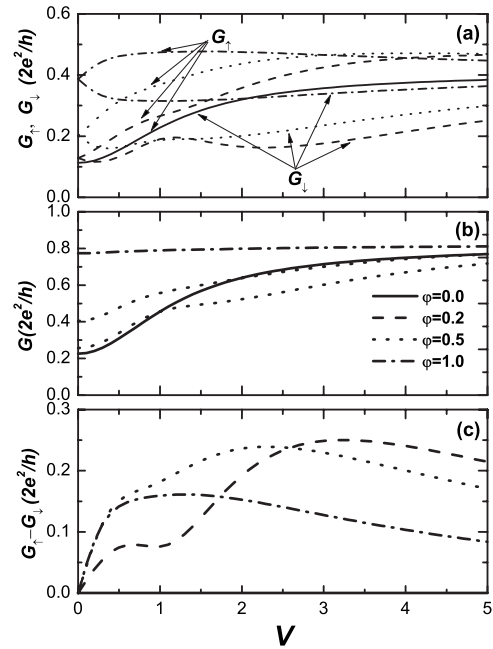


FIG. 4. (a) The conductance components G_\uparrow and G_\downarrow , (b) the total conductance G , and (c) the polarized conductance $G_\uparrow - G_\downarrow$ versus the bias V for $\varphi=0.0, 0.2, 0.5$, and 1.0 . The other parameters are $U=5.0$, $t_{LR}=0.2$, and $\epsilon_d=-2.5$.

one conductance peak in the $G_p \sim V$ curve. As φ increases further, the conductance difference contributed from spin-up and spin-down transport electrons begins to decrease.

To investigate the effect of Rashba SOI on the Fano resonance peaks and Kondo effect, Figs. 5 and 6 show the spin-

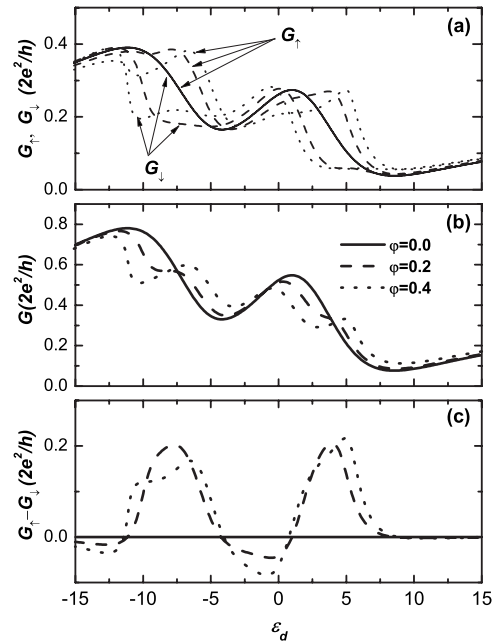


FIG. 5. (a) The conductance components G_\uparrow and G_\downarrow , (b) the total conductance G , and (c) the polarized conductance $G_\uparrow - G_\downarrow$ versus the dot level ϵ_d for $\varphi=0.0, 0.2$, and 0.4 . The other parameters are $U=5.0$, $t_{LR}=0.1$, and $V=3.0$.

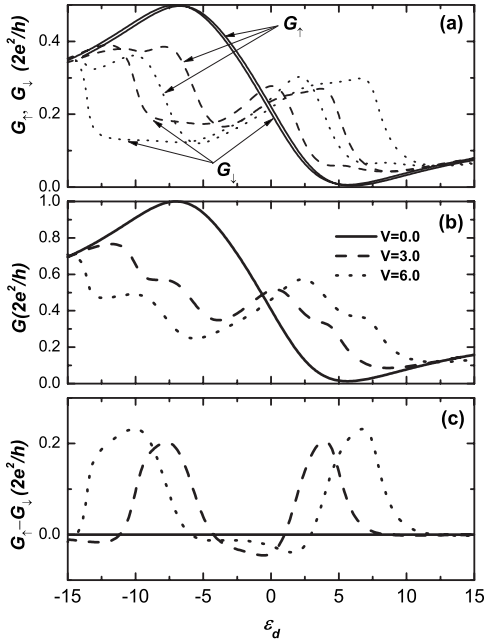


FIG. 6. (a) The conductance components G_{\uparrow} and G_{\downarrow} , (b) the total conductance G , and (c) the polarized conductance $G_{\uparrow} - G_{\downarrow}$ versus the dot level ϵ_d for $V=0.0, 3.0,$ and 6.0 . The other parameters are $U=5.0, t_{LR}=0.1,$ and $\varphi=0.2$.

dependent conductance G_s , total conductance G , and the polarized conductance $G_p = G_{\uparrow} - G_{\downarrow}$ versus the QD level ϵ_d for different Rashba interaction strengths φ and bias voltages V , respectively. Figure 5(a) indicates that the spin-resolved conductance G_s shifts horizontally in the presence of Rashba SOI, similar to the case in one-dimensional nanowire.³³ Compared with the case in the absence of Rashba SOI, two new peaks appear on both sides of the Kondo peak while the Kondo peak decreases with the increase of the bias V . As shown in Fig. 6, the Fano resonance peaks of the total conductance G are deformed more seriously for higher V . In the nonequilibrium case $V \neq 0$, the polarized conductance G_p appears and shows nonmonotonic change as a function of ϵ_d and two peaks appear on two sides of $\epsilon_d = -U/2$. The positions of the two peaks move farther away with the increase of the bias V . It is interesting that both the total conductance G and the polarized conductance G_p indicate the splitting of the Kondo peak and deformation of the Fano-Kondo plateau, which is due to the lifting of the spin degeneracy induced by the Rashba SOI. From the above discussion, the most direct evidence to prove the effects of Rashba SOI is that more dips are expected to appear in the Fano-type conductance. Actually, in the experiments,¹³ it has been shown that some small ripples are observed in the conductance, which may be the results induced by SOI.

C. Shot noise and the Fano factor

In this section, we investigate the effect of Rashba SOI on the zero-frequency shot noise of the charge current and the corresponding Fano factor. The charge current correlation is $\mathcal{S}(t, t') = \langle \{\hat{\Delta}I(t), \hat{\Delta}I(t')\} \rangle$, where $\hat{I}(t) = [\hat{I}_L(t) - \hat{I}_R(t)]/2$; thus,

$\mathcal{S} = \frac{1}{4}(\mathcal{S}_{LL} + \mathcal{S}_{RR} - \mathcal{S}_{LR} - \mathcal{S}_{RL})$. Due to current conservation, for the two terminal system, there is $\mathcal{S}_{LL} = \mathcal{S}_{RR} = -\mathcal{S}_{LR} = -\mathcal{S}_{RL}$ in the zero frequency. In the following, we use the component $\mathcal{S}_{LL} = \sum_{\sigma\sigma'} \mathcal{S}_{LL}^{\sigma\sigma'} = \mathcal{S}_{LL}^{\uparrow\uparrow} + \mathcal{S}_{LL}^{\downarrow\downarrow} + 2\mathcal{S}_{LL}^{\uparrow\downarrow} \equiv \mathcal{S}$ to represent the noise of charge current and then the Fano factor is given by $\gamma = \mathcal{S}/2eI$. Under the slave boson approach, the model Hamiltonian [Eq. (1)] reduces to a noninteracting quadratic one [Eq. (5)], which means that $\mathcal{S}_{LL}^{\uparrow\downarrow} = 0$ at this mean-field level.²⁴ Both the average current and the current fluctuation can be expressed in terms of the transmission coefficient. From Wick's theorem, for the current fluctuation in the limit of zero temperature, only shot noise exists and the expression can be simplified as²³

$$\mathcal{S}_{LL}^{ss} = \frac{2e^2}{h} \int d\omega T_s(\omega)[1 - T_s(\omega)]. \quad (20)$$

The Kondo effects on the current fluctuation in different types of QD systems are well studied.^{19–25} The numerical results show that the Kondo effect always reduces the Fano factor in a single QD,²¹ while in the double QD system, the Fano factor sensitively relies on the configuration of the QDs and the coupling parameter between two dots.²⁴ Moreover, the shot noise for the system of an AB ring embedded with a common QD has also been investigated in detail.²² It is shown that the shot noise indicates more information about the interference, which cannot be seen in the average current.

Now, we first consider the case in the absence of the Rashba SOI, which is shown in Fig. 7. Figure 7(a) plots the Fano factor γ as a function of bias voltage V for different direct coupling strengths $t_{LR} = 0.0, 0.1, 0.2,$ and 0.5 . If there is no direct tunneling $t_{LR} = 0.0$, the Fano factor is suppressed completely ($\gamma = 0$) in the Kondo regime in the linear response regime $V = 0$. In this case, it has been pointed out that the property $\gamma = 1/2$ is universal in the limit of $V \rightarrow \infty$ whether the Coulomb interactions are present or not.¹⁶ However, with the presence of the direct tunneling t_{LR} between two leads, the Fano factor γ in the limit of $V \rightarrow \infty$ can be tuned by t_{LR} and still not related to the strength of the Coulomb interactions [as shown in Fig. 7(b)]. The reason is that $\gamma = 1/2$ in the large V limit is only expected for a symmetric structure, while there are two asymmetric paths in the present AB ring device. It is also shown in Figs. 7(c) and 7(d) that the bias voltage can increase or suppress the Fano factor, which depends on the energy level in the QD and the direct coupling strength t_{LR} . Corresponding to the appearance of the Kondo conductance peak near the Fermi energy induced by the finite bias, the Fano factor near $\epsilon_d = 0$ is suppressed by the bias.

In the following, we study the effect of Rashba SOI φ on the shot noise and the corresponding Fano factor for different sets of coupling parameters. Figures 8(a) and 8(b) show the shot noise components $\mathcal{S}_{\uparrow\uparrow}, \mathcal{S}_{\downarrow\downarrow}$ and the total shot noise \mathcal{S} versus the dot level ϵ_d for different Rashba SOIs $\varphi = 0.0, 0.2,$ and 0.4 . For the lifting of the spin degeneracy, $\mathcal{S}_{\uparrow\uparrow}$ and $\mathcal{S}_{\downarrow\downarrow}$ are split by the Rashba SOI. It is shown in Fig. 8(b) that the total shot noise increases with the increase of Rashba SOI for broad range of ϵ_d . Figures 8(c) and 8(d) indicate that the

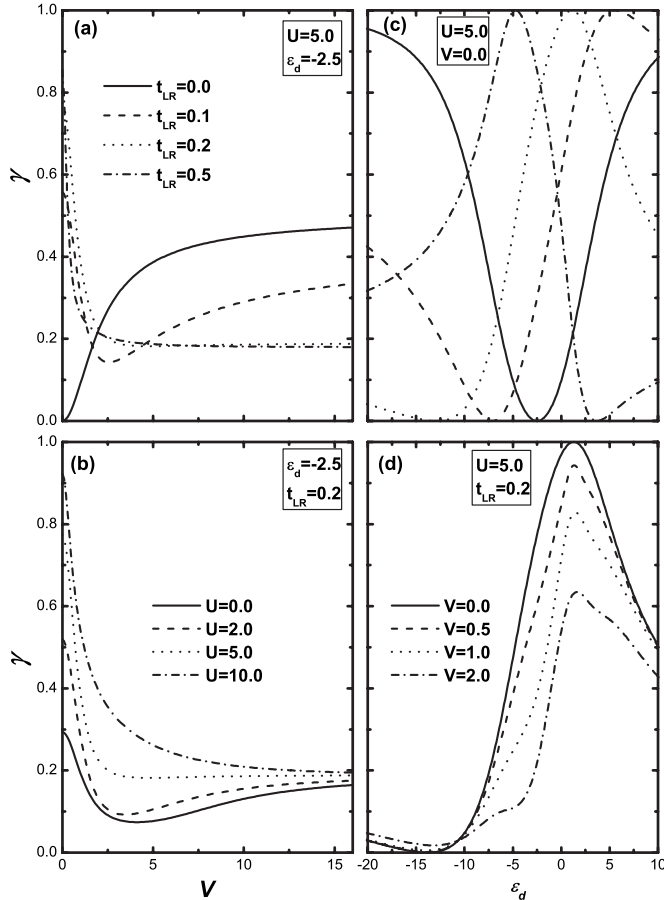


FIG. 7. [(a) and (b)] The Fano factor γ versus the bias V for different direct couplings t_{LR} and Coulomb interactions U in the absence of Rashba SOI ($\varphi=0$). (a) $t_{LR}=0.0, 0.1, 0.2,$ and 0.5 . $U=5.0$ and $\epsilon_d=-2.5$. (b) $U=0.0, 2.0, 5.0,$ and 10.0 . $U=5.0$ and $t_{LR}=0.2$. [(c) and (d)] The Fano factor γ versus the dot level ϵ_d for different direct couplings t_{LR} and biases V . (c) $t_{LR}=0.0, 0.1, 0.2,$ and 0.5 . $U=5.0$ and $V=0.0$. (d) $V=0.0, 0.5, 1.0,$ and 2.0 . $U=5.0$ and $t_{LR}=0.2$.

Rashba SOI φ can increase or decrease the Fano factor, which depends on the bias voltage qualitatively. When the dot level ϵ_d is higher than the chemical potentials in both leads, the Rashba SOI decreases the Fano factor, while the Fano factor increases for $\epsilon_d < \mu_L$. The feature is quite different from that caused by the magnetic field, though both of them break the spin degeneracy. The magnetic field enhances the Fano factor in a QD system²¹ that can be interpreted as the fact that due to application of magnetic fields in the QD, reduction of the Kondo-enhanced density of states decreases the conductance or the transmission probability in the Kondo regime. However, the Rashba SOI can increase or suppress the Fano factor, as shown in Figs. 8(c) and 8(d). When the dot level is above the chemical potentials in both leads, electrons are difficult to transmit through the QD and the shot noise is nearly Poissonian, but the Rashba SOI can help the spin-up electrons to tunnel through the QD. In this case, correlation of the tunneling events can be enhanced and the Fano factor decreases in the presence of Rashba SOI. When

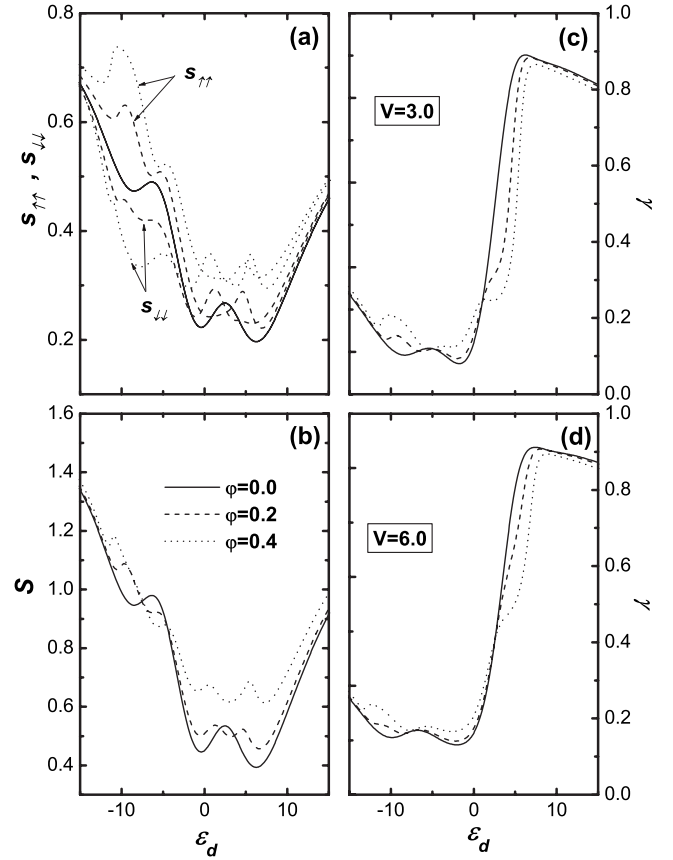


FIG. 8. (a) The shot noise components $S_{\uparrow\uparrow}$ and $S_{\downarrow\downarrow}$ and (b) the total shot noise S versus the dot level ϵ_d for $\varphi=0.0, 0.2,$ and 0.4 . $V=3.0$. [(c) and (d)] The Fano factor γ versus the dot level ϵ_d for $V=3.0$ and $V=6.0$, respectively. The other parameters are $U=5.0$ and $t_{LR}=0.1$.

the dot level is below the chemical potentials, the Rashba SOI induces spin accumulation in the QD, which makes spin-down electrons difficult to tunnel through the QD. Therefore, the Rashba SOI destroys the correlation in this case and then the Fano factor increases.

IV. SUMMARY

In summary, by using the finite- U slave-boson approach, we study the Kondo effect on the spin accumulation, spin-dependent transport, and noise properties in a QD which contains the Rashba SOI. The spin accumulation shows two asymmetric peaks as a function of dot level ϵ_d around $-U/2$, and the peak value at higher ϵ_d is larger due to the lower possibility of doubly occupied state. The Rashba SOI induces two more conductance peaks on both sides of the Kondo peak in the Fano-type conductance, while the Kondo peak is suppressed at the same time. Experimentally, more conductance dips caused by Rashba SOI are expected to appear in the Fano-type conductance, which can be realized in the present technology. Furthermore, for the relatively large bias voltage, the Fano-type conductance can be deformed seriously while the Kondo peak is less deformed. For the spin-polarized conductance ($G_{\uparrow} - G_{\downarrow}$), two peaks also appear

which locates two sides of $\epsilon_d = -U/2$ and the locations of the two peaks are determined by the bias voltage.

The effect of the Rashba SOI on the noise properties is also discussed. The noise components $S_{\uparrow\uparrow}$ and $S_{\downarrow\downarrow}$ are split by the Rashba SOI and the total shot noise increases with the increase of Rashba SOI for the wide range of ϵ_d . In the large bias voltage limit, the Fano factor is equal for different Coulomb interactions but can be tuned by the direct coupling between two leads. Similar to the magnetic field, the Rashba SOI can also lift the spin degeneracy. However, the magnetic field always enhances the Fano factor, while the Rashba SOI can increase or decrease it, depending on the dot level and the chemical potentials in both leads. When the dot level is above the chemical potentials in both leads, the spin broken symmetry induced by Rashba SOI weakens the destructive interference, which enhances the correlation of the tunneling processes and the Fano factor decreases. When the dot level is below the chemical potentials, effects of the Rashba SOI are dominated by the tunneling events that a spin-down electron is difficult to tunnel through the QD. Therefore, the Rashba SOI destroys the correlation and then the Fano factor increases.

ACKNOWLEDGMENTS

This project was supported by the National Natural Science Foundation of China (No. 10474052), by Tsinghua Basic Research Foundation (No. Jcpy2005058), by Specialized Research Fund for the Doctoral Program of Higher Education (No. 2006003047), and by the 973 Program (No. 2006CB605105).

APPENDIX

In this appendix, we give the concise derivation of the second-quantized Hamiltonian [Eq. (1)] and discuss the effect of the matrix Berry phase on a multilevel QD which contains Rashba SOI. In the real space, the single-particle Hamiltonian of the QD can be given by

$$H_s(\mathbf{r}) = \frac{p_x^2 + p_z^2}{2m^*} + V(\mathbf{r}) + \hat{\sigma} \cdot \mathbf{M}(\mathbf{r}) + H_{R1} + H_{R2}. \quad (\text{A1})$$

H_s contains the kinetic and potential energies, the interaction energy with the magnetic moment \mathbf{M} in the ferromagnetic leads, and the Rashba SOI $H_{R1} + H_{R2}$, where $H_{R1} = \alpha_R(\hat{\sigma}_z p_x + \hat{\sigma}_x p_z)/2\hbar$ and $H_{R2} = -\alpha_R \hat{\sigma}_x p_z/\hbar$. It is noted that in real space, H_{R1} induces a spin precession, while H_{R2} leads to the intersubband mixing. During second quantizing the Rashba SOI, the unitary transformation with the following unitary matrix is used,⁶

$$u(x) = \begin{cases} 1, & x < x_L \\ \exp[-i\hat{\sigma}_z k_R(x - x_L)], & x_L < x < x_R \\ \exp[-i\hat{\sigma}_z k_R(x_R - x)], & x_R < x, \end{cases} \quad (\text{A2})$$

where $k_R = \alpha_R m^*/\hbar^2$. Here, the Rashba SOI strength α_R is zero outside of the QD ($x_R < x$ or $x < x_L$, see Fig. 9). It is equivalent to choose a space-dependent spin coordinate. In the rotating frame which follows the spin precession, the

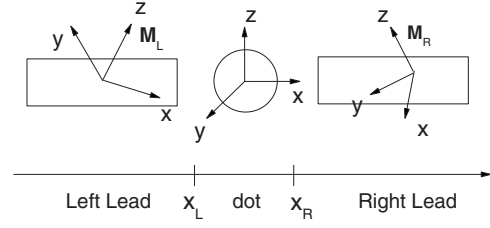


FIG. 9. Schematic diagram for a metal-QD-metal device configuration where the QD is weakly coupled to both the leads. The Rashba SOI exists in the central QD region (i.e., $\alpha_R \neq 0$ for $x_L < x < x_R$). The vector $\mathbf{M}_{L(R)}$ denotes the permanent magnetic moments in the left (right) lead.

spin is invariant. Under this unitary transformation, H_s of Eq. (A1) becomes

$$H'_s = u(x)^\dagger H_s u(x) = \frac{p_x^2 + p_z^2}{2m^*} + V(\mathbf{r}) - \frac{\hbar^2 k_R^2}{2m^*} + \sigma \cdot \mathbf{M}'(\mathbf{r}) + H'_{R2}, \quad (\text{A3})$$

where $\mathbf{M}'_L = \mathbf{M}_L$ and $|\mathbf{M}'_R| = |\mathbf{M}_R|$, but the directional angles of \mathbf{M}'_R are changed to $(\theta_R, \phi_R - 2\phi_{so})$, with $\phi_{so} = k_R L$. For the normal metal leads, there are $\theta_R = 0$ and $\phi_R = 0$. The second-quantized form of H'_{R2} is

$$H'_{R2} = \sum_{m,n} t_{mn}^{so} c_{dm\downarrow}^\dagger c_{dn\uparrow} + \text{H.c.}, \quad (\text{A4})$$

where $t_{mn}^{so} = \langle ms' | H'_{R2} | ns \rangle$. For $s' = s$, this matrix element is exactly zero. For the nondiagonal matrix elements, it can be proved that $t_{mn}^{so} = -t_{nm}^{so}$. This interlevel spin-flip coupling is similar to the intersubband mixing in real space.^{7,8} Despite the interlevel spin flips, the system is still at least twofold degenerate for any eigenstates because $t_{mn}^{so} = -t_{nm}^{so}$. Hence, the second-quantized form for the Hamiltonian (A1) of the metal-QD-metal device can be written as⁶

$$H = \sum_{\alpha,k,s} \epsilon_{\alpha k} c_{\alpha ks}^\dagger c_{\alpha ks} + \sum_{n,s} \epsilon_n c_{dns}^\dagger c_{dns} + \sum_{ns,ms'} U \hat{n}_{dns} \hat{n}_{dms'} + \sum_{m,n} (t_{mn}^{so} c_{dm\downarrow}^\dagger c_{dn\uparrow} + \text{H.c.}) + \sum_{\alpha,k,n,s} (t_{\alpha kn} c_{\alpha ks}^\dagger e^{-isk_R x} c_{\alpha kns} + \text{H.c.}). \quad (\text{A5})$$

In the second-quantized Hamiltonian, H_{R1} embodies its effect in the extra spin-resolved phase in the hopping constant between the leads and the QD, and H_{R2} causes spin flips between different energy levels.

Considering the harmonic potentials in the QD, a finite external voltage with the form $V_b = \epsilon' x$ (ϵ' can be varied electrically) provides a distortion of the harmonic potentials and does not cause a spin flip but an interlevel electronic flip. When the distortion potential and the energy scale $E_R = \alpha_R/L$ are comparable with the energy spacing between the QD levels, considerable magnitude of matrix Berry phases can be produced and it represents the mixing between different degenerate levels in the QD.⁷ The typical value Γ of the coupling strength between the QD and the leads is of order $10 \mu\text{eV}$.¹¹⁻¹⁴ The bias voltage discussed here is of order

$1-10\Gamma$, which is much smaller than the typical values of the energy spacing (of order $1-10$ meV) between the QD levels. Therefore, when the applied bias voltage is relatively low or the dot-lead coupling is relatively weak, the second-

quantized Hamiltonian [Eq. (1)] can be considered as a good approximation. In our work, only single energy level is considered and so the Rashba SOI embodies its effect in the extra spin-resolved phase in H_T .

*lvhf04@mails.tsinghua.edu.cn

†guoy66@tsinghua.edu.cn

- ¹I. Zutic, J. Fabian, and S. Das Sarma, *Rev. Mod. Phys.* **76**, 323 (2004).
- ²D. Loss and D. P. DiVincenzo, *Phys. Rev. A* **57**, 120 (1998); P. Recher, E. V. Sukhorukov, and D. Loss, *Phys. Rev. Lett.* **85**, 1962 (2000).
- ³A. Imamoglu, D. D. Awschalom, G. Burkard, D. P. DiVincenzo, D. Loss, M. Sherwin, and A. Small, *Phys. Rev. Lett.* **83**, 4204 (1999).
- ⁴G. Schmidt, D. Ferrand, L. W. Molenkamp, A. T. Filip, and B. J. van Wees, *Phys. Rev. B* **62**, R4790 (2000).
- ⁵R. Ionićoiu and I. D'Amico, *Phys. Rev. B* **67**, 041307(R) (2003); G. Usaj and C. A. Balseiro, *Europhys. Lett.* **72**, 631 (2005).
- ⁶Q. F. Sun, J. Wang, and H. Guo, *Phys. Rev. B* **71**, 165310 (2005); Q. F. Sun and X. C. Xie, *ibid.* **73**, 235301 (2006).
- ⁷S.-R. Eric Yang and N. Y. Hwang, *Phys. Rev. B* **73**, 125330 (2006).
- ⁸S.-R. Eric Yang, *Phys. Rev. B* **74**, 075315 (2006); arXiv:cond-mat/0701318.
- ⁹U. Fano, *Phys. Rev.* **124**, 1866 (1961).
- ¹⁰A. C. Hewson, *The Kondo Problem to Heavy Fermions* (Cambridge University Press, Cambridge, 1993).
- ¹¹D. Goldhaber-Gordon, H. Shtrikman, D. Mahalu, D. Abusch-Magder, U. Meirav, and M. A. Kastner, *Nature (London)* **391**, 156 (1998); S. M. Cronenwett, T. H. Oosterkamp, and L. P. Kouwenhoven, *Science* **281**, 540 (1998).
- ¹²W. G. van der Wiel, S. De Franceschi, T. Fujisawa, J. M. Elzerman, S. Tarucha, and L. P. Kouwenhoven, *Science* **289**, 2105 (2000); Y. Ji, M. Heiblum, D. Sprinzak, D. Mahalu, and H. Shtrikman, *ibid.* **290**, 779 (2000).
- ¹³K. Kobayashi, H. Aikawa, A. Sano, S. Katsumoto, and Y. Iye, *Phys. Rev. B* **70**, 035319 (2004).
- ¹⁴M. Sato, H. Aikawa, K. Kobayashi, S. Katsumoto, and Y. Iye, *Phys. Rev. Lett.* **95**, 066801 (2005); S. Katsumoto, M. Sato, H. Aikawa, and Y. Iye, *Physica E (Amsterdam)* **34**, 36 (2006).
- ¹⁵B. R. Bulka and P. Stefański, *Phys. Rev. Lett.* **86**, 5128 (2001).
- ¹⁶W. Hofstetter, J. König, and H. Schoeller, *Phys. Rev. Lett.* **87**, 156803 (2001).
- ¹⁷J. Takahashi and S. Tasaki, *J. Phys. Soc. Jpn.* **75**, 094713 (2006); I. Maruyama, N. Shibata, and K. Ueda, *Physica B* **378-380**, 938 (2006).
- ¹⁸R. López, D. Sanchez, and L. Serra, arXiv:cond-mat/0610515; D. Sanchez and L. Serra, *Phys. Rev. B* **74**, 153313 (2006); L. Serra and D. Sanchez, *J. Phys.: Conf. Ser.* **61**, 1037 (2007); F. Chi and S. S. Li, *J. Appl. Phys.* **100**, 113703 (2006).
- ¹⁹Ya. M. Blanter and M. Büttiker, *Phys. Rep.* **336**, 2 (2000).
- ²⁰V. V. Kuznetsov, E. E. Mendez, J. D. Bruno, and J. T. Pham, *Phys. Rev. B* **58**, R10159 (1998).
- ²¹B. Dong and X. L. Lei, *J. Phys.: Condens. Matter* **14**, 4963 (2002).
- ²²J. Takahashi and S. Tasaki, *J. Phys. Soc. Jpn.* **74**, 261 (2005).
- ²³S.-R. Eric Yang, *Solid State Commun.* **81**, 375 (1992); A. Shimizu and M. Ueda, *Phys. Rev. Lett.* **69**, 1403 (1992); B. Kubala and J. König, *Phys. Rev. B* **65**, 245301 (2002).
- ²⁴R. López, R. Aguado, and G. Platero, *Phys. Rev. B* **69**, 235305 (2004).
- ²⁵A. Golub, *Phys. Rev. B* **73**, 233310 (2006); G. B. Zhang, S. J. Wang, and L. Li, *ibid.* **74**, 085106 (2006).
- ²⁶D. Sanchez, R. López, and M.-S. Choi, *J. Supercond.* **18**, 251 (2005).
- ²⁷G. Kotliar and A. E. Ruckenstein, *Phys. Rev. Lett.* **57**, 1362 (1986).
- ²⁸B. Dong and X. L. Lei, *Phys. Rev. B* **63**, 235306 (2001); *J. Phys.: Condens. Matter* **13**, 9245 (2001).
- ²⁹P. Coleman, *Phys. Rev. B* **29**, 3035 (1984).
- ³⁰G. H. Ding and B. Dong, *Phys. Rev. B* **67**, 195327 (2003); Y. Takagaki and K. H. Ploog, *Phys. Status Solidi B* **242**, 3155 (2005).
- ³¹B. Dong, G. H. Ding, H. L. Cui, and X. L. Lei, *Europhys. Lett.* **69**, 424 (2005); G. H. Ding, C. K. Kim, and K. Nahm, *Phys. Rev. B* **71**, 205313 (2005).
- ³²J. Ma and X. Lei, *Europhys. Lett.* **67**, 432 (2004).
- ³³Y. X. Li, Y. Guo, and B. Z. Li, *Phys. Rev. B* **72**, 075321 (2005).